Innovative Stacking Method for Enhanced Data Fusion in Pollutant Population Risk Evaluation

Yudie Jianyao[a,b], Xiaole Zhang[a,b], Hongyong Yuan[a,b], Guofeng Su [a,b]
[a] School of Safety Science, Tsinghua University, Beijing 100084, China
[b] Institute of Public Safety Research, Tsinghua University, Beijing 100084, China

Abstract: Air pollution, particularly particulate matter (PM), has become a critical global public health concern. PM_{10} and $PM_{2.5}$ are especially significant due to their severe health impacts. Accurate assessment of $PM_{2.5}$ and PM_{10} exposure with high spatial and temporal resolution is essential for evaluating health effects. In this study, we developed a High-Resolution Particulate Matter Estimation via Trained Stacking (HR-PM-TS) model to estimate the distribution of PM with high spatial (1 km × 1 km) and temporal (hourly) resolutions. By using stacking to downscale and integrate station and grid data, significantly improved the PM prediction ability. The Stacking method notably enhances computational efficiency, reducing prediction times by an average of 20 times compared to deep learning models. Our analysis included examining population-weighted PM levels against the World Health Organization's Air Quality Guideline levels across different age groups, revealing differing trends for PM_{10} and $PM_{2.5}$. Population-weighted PM levels generally showed an increase, with 66% of areas for $PM_{2.5}$ and 56% of areas for PM_{10} experiencing higher concentrations when compared to unweighted PM. Additionally, we investigated the correlation between population-weighted PM and various land cover types, finding significant correlations with Built-Up and Crops. This indicates that regions with more human and agricultural activities tend to have higher PM concentrations, suggesting a direct impact of land use on air quality. In conclusion, the findings of this study are invaluable for developing effective environmental and health policies. By enhancing the understanding of the relationship between particulate matter, population distribution, and land cover, this research offers critical insights for policymakers to devise targeted strategies aimed at mitigating the impact of air pollution on public health, especially in densely populated and high-risk areas.

Keywords: Particulate Matter (PM), Machine Learning Techniques, Stacking Method, Population Health Risk Analysis

1. INTRODUCTION

Air pollution, particularly particulate matter (PM), poses significant risks to public health, contributing to respiratory and cardiovascular diseases, as well as premature mortality [1-4]. $PM_{2.5}$ (particles with a diameter of less than 2.5 micrometers) and PM_{10} (particles with a diameter of less than 10 micrometers) are of particular concern due to their ability to penetrate deep into the respiratory system [5]. Understanding the distribution and concentration of these pollutants is crucial for effective air quality management and public health protection.

Obtaining high-resolution PM data is challenging. Machine learning techniques are increasingly used to estimate PM concentrations by combining satellite data and station observations [6]. For instance, to estimate daily $PM_{2.5}$ at 1×1 km^2 resolution, Allan et al. applied extreme gradient boosting (XGBoost) in the Northeastern USA from 2000 to 2015 [7]. Similarly, M. Ghahremanloo et al. used MAIAC AOD and a random forest model to estimate daily $PM_{2.5}$ levels in Texas from 2014 to 2018 [8]. Chen et al. developed an improved random forest (IRF) model for Shenzhen, China, for the years 2016-2018 [9], and Zhang et al. applied a random forest approach in South Africa [10].

To enhance generalization and prediction accuracy, stacking methods have been employed. For example, Danesh et al. used ensemble-averaged predictions with a generalized additive model (GAM) for daily $PM_{2.5}$ in London [11]. Yu et al. implemented deep ensemble machine learning (DEML) to estimate global daily ambient $PM_{2.5}$ concentrations at a 0.1° × 0.1° spatial resolution from 2000 to 2019 [12].

In this study, we propose a novel approach to high-resolution particulate matter estimation via a trained stacking model (HR-PM-TS). Our model predicts hourly $PM_{2.5}$ and PM_{10} concentrations, providing finer

temporal resolution than previous studies. Furthermore, we integrate population data and land cover types, enabling a comprehensive analysis of exposure risks. This approach allows us to assess PM concentrations against both 24-hour and annual World Health Organization (WHO [13]) Air Quality Guideline (AQG) levels, offering a detailed evaluation of air quality impacts on different population groups and land cover scenarios. Our objectives are to:

1. Develop a high-resolution PM estimation model using a trained stacking approach.
2. Analyze the spatial distribution of $PM_{2.5}$ and PM_{10} across different administrative areas.
3. Assess the exposure risk to different age groups, focusing on vulnerable populations such as children and the elderly.
4. Investigate the correlation between PM concentrations and various land cover types.

By providing a detailed analysis of PM distribution and its impact on different population groups, this study aims to contribute to the development of targeted air quality management strategies that can effectively mitigate the adverse health effects of air pollution.

2. Method

2.1. Study Area and Dataset

In this study, we focus exclusively on Switzerland at a national level. Switzerland adopts a proactive approach to developing air quality policies, ensuring that its environmental standards meet or exceed all European requirements [14]. Although pollution levels on the entire European continent are among the lowest globally, Switzerland's air quality is among the best in Europe, reflecting the country's long-term strategy [15]. Hence, analyzing PM in Switzerland helps determine the extent to which they meet WHO AQG levels.

Temporal data on PM with particle diameters between 5 nm and 3 µm has been available since 2005 through the National Air Pollution Monitoring Network (NABEL). Five stations have been selected: Basel-Binningen (BAS, suburban, background), Bern-Bollwerk (BER, urban, roadside), Härkingen-A1 (HAE, rural, adjacent to a motorway), Lugano-University (LUG, urban, background), and Rigi-Seebodenalp (RIG, rural, altitude > 1000 m), all equipped with long-term PM measurements from the Swiss NABEL.

Annually, the Copernicus Atmosphere Monitoring Service (CAMS [16]) produces regional air quality reanalyses for the European domain at a resolution of 0.1 degrees (approximately 10 km) from 2003 to 2023. The Copernicus Climate Data is based on ERA5-Land [17] Hourly Data and provides global horizontal coverage at a resolution of 0.1° × 0.1° with temporal coverage from January 1950 to the present. Traffic data is obtained from the Open Transport Map, and population data is accessible from the Gridded Population of the World (GPW), v4 [18]. The land cover fraction data is sourced from the Copernicus Global Land Service: Land Cover 100m, collection 3, epoch 2019: Globe [19, 20]. This dataset provides versatile cover fractions, representing the percentage (%) of ground cover for the 10 main classes, with a spatial resolution of 100 meters. And the code can be found at https://github.com/Jyyd/PM_con_Estimate.

2.2. The Structure of Stacking

The stacking method consists of two layers: the base learner (first layer) and the meta learner (second layer). For $PM_{2.5}$ prediction, the first layer includes K-Nearest Neighbors (KNN), Random Forest (RF), LightGBM (LGB), and Gradient Boosting Regressor (GBR). The second layer employs a Multi-Layer Perceptron (MLP), as demonstrated in formula (1). For PM_{10} prediction, the first layer comprises LGB and GBR, with a MLP serving as the meta learner in the second layer, as illustrated in formula (2).

$$\hat{y}_{PM_{2.5}} = f_{MLP}\left\{\left[f_{KNN}(X)\, f_{RF}(X)\, f_{LGB}(X)\, f_{GBR}(X)\right]_{\text{First Layer}}\right\}_{\text{Second Layer}} \tag{1}$$

$$\hat{y}_{PM_{10}} = f_{MLP}\left\{\left[f_{LGB}(X)\, f_{GBR}(X)\right]_{\text{First Layer}}\right\}_{\text{Second Layer}} \tag{2}$$

To compare with the HR-PM-TS, four model types are divided in Table 1. Linear Models include Linear Regression and Lasso Regression. Neighbor-based Models comprise K-Nearest Neighbors (KNN). Tree-based Models consist of Decision Tree, Random Forest, AdaBoost, Gradient Boosting, and Light Gradient-Boosting Machine (LightGBM). Deep Learning Models encompass Recurrent Neural Network (RNN), Convolutional Neural Network (CNN), and Long Short-Term Memory (LSTM).

Table 1. Model Category

Model Type	The Models in Model Type
Linear Models	Linear Regression
	Lasso Regression
Neighbor-based Models	K-Nearest Neighbors (KNN)
Tree-based Models	Decision Tree
	Random Forest
	AdaBoost
	Gradient Boosting
	Light Gradient-Boosting Machine (LightGBM)
Deep Learning Models	Recurrent Neural Network (RNN)
	Convolutional Neural Network (CNN)
	Long Short-Term Memory (LSTM)
HR-PM-TS	Stacking

2.3. Prediction metrics in HR-PM-TS

Details of the metrics formulas presented in this study: Root Mean Square Error (RMSE), Mean Absolute Error (MAE) and R^2 score (coefficient of determination) can be found in Scikit-learn [21]. And for the Mean Bias (M-Bias):

$$M\text{-}Bias = \frac{1}{n}\sum_{i=1}^{n}(\hat{y}_i - y_i) \tag{3}$$

Note: where y_i is the actual observation, $\hat{y}_i$ is the predicted value of the model. To compare models, adjust the *bias* in model selection and evaluation [22] to the Mean Bias.

3. Results and Discussion

3.1. An Approach to High-Resolution Particulate Matter Estimation via Trained Stacking

This study presents a method for estimating high-resolution particulate matter (PM) using a trained stacking model (HR-PM-TS). The feature set includes temporal data collected from NABEL stations, low-resolution grid data from CAMS (including $PM_{2.5}$, PM_{10}, NO_X, NO_2, and Ozone), and meteorological data from ERA5 (including wind speed, temperature, radiation, relative humidity, and precipitation). Additionally, traffic data (traffic volume) and time-related data (hour, month, weekday) are incorporated into the feature set.

To develop the trained stacking model, the data fusion dataset is split into a training set (from 2016 to 2019, comprising 78% of the data) and a testing set (for the year 2020, comprising 22% of the data). As shown in Figure 1, scatter plots compare the measurements and predictions of $PM_{2.5}$ and PM_{10} for daily and monthly results. For $PM_{2.5}$ (in Figure 1 (a) and (c)), an increase in the time scale from days to months improves the metrics: the daily R^2 is 0.94, while the monthly R^2 is 0.97. The RMSE decreases from 1.47 (daily) to 0.66 (monthly), and the MAE decreases from 0.92 (daily) to 0.48 (monthly). Similarly, for PM_{10} (in Figure 1 (b) and (d)), the R^2 increases from 0.91 (daily) to 0.97 (monthly). The RMSE decreases from 2.46 (daily) to 0.99 (monthly), and the MAE decreases from 1.30 (daily) to 0.75 (monthly). The increase in R^2 indicates an improvement in predictive ability, while the decrease in RMSE and MAE suggests enhanced prediction accuracy and precision.

The M-Bias metric indicates the generalization ability of the model. It is important to note that the RIG station's daily results for $PM_{2.5}$ and PM_{10} are outlined by the 0.5- and 2-times red lines. This station, being

the lowest bound for the dataset with an altitude higher than 1000 meters, shows different characteristics compared to other stations. Despite this, the data from other stations fit well.

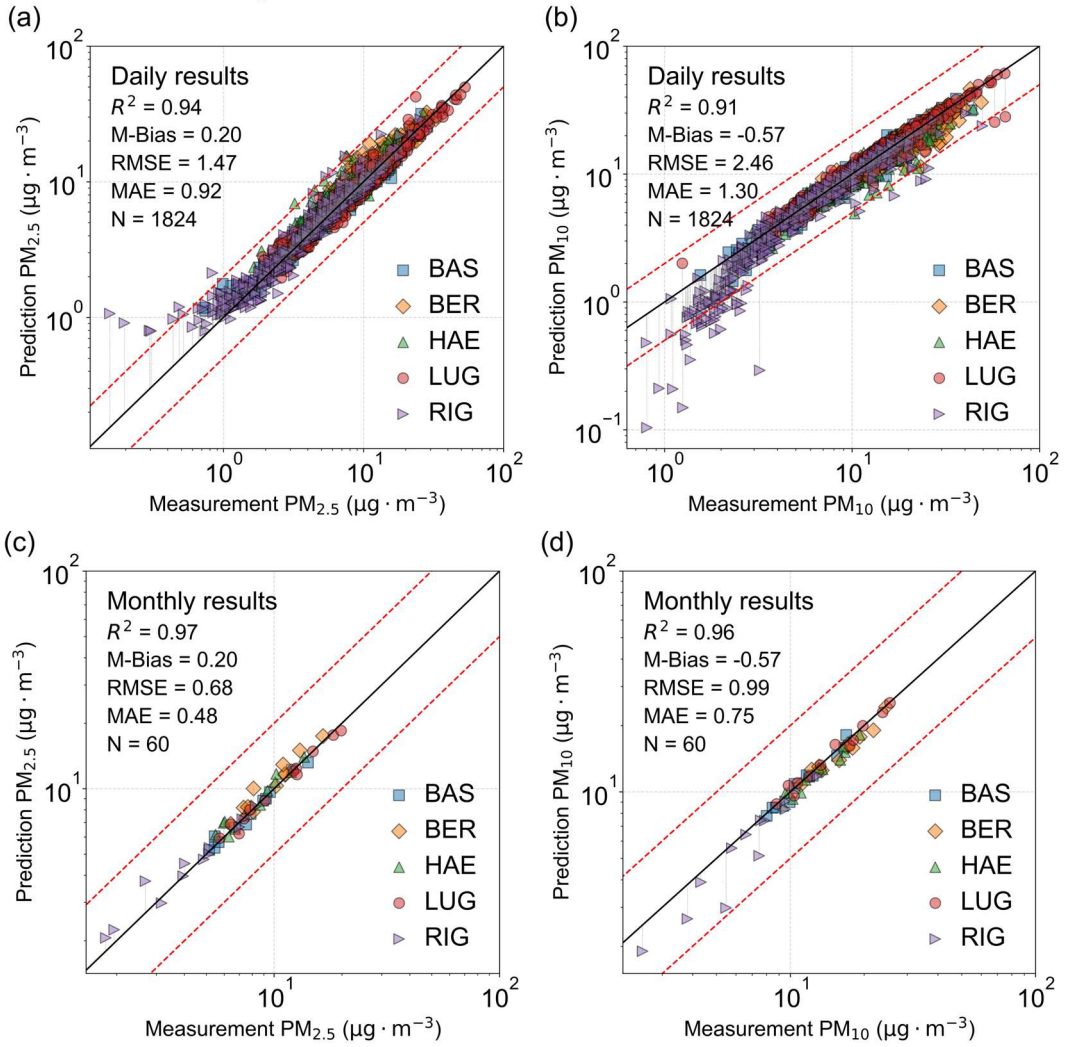

Figure 1. The scatter plot between measurement and prediction of $PM_{2.5}$ and PM_{10} in daily (N = 1824) and monthly (N = 60) results

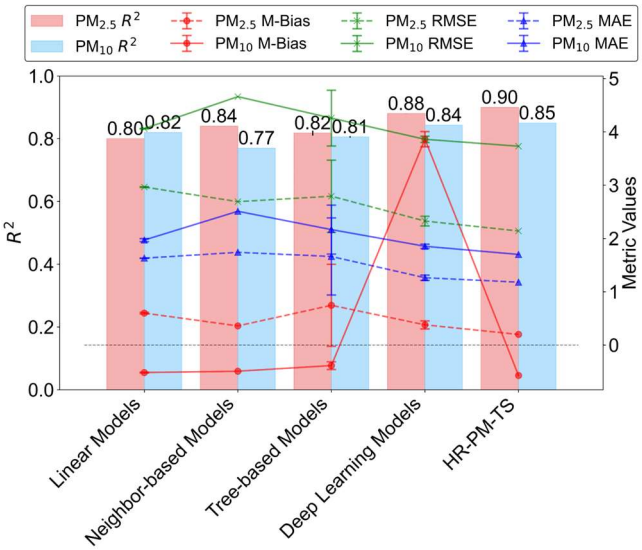

Figure 2. Results and Performance of High-Resolution Particulate Matter Estimation via Trained Stacking (HR-PM-TS) compare with other model types

In Figure 2, the performance metrics for $PM_{2.5}$ indicate that the HR-PM-TS model provides superior prediction accuracy, with an R^2 of 0.90, an RMSE of 2.14, and an MAE of 1.17. Additionally, it exhibits the best generalization ability with an M-Bias of 0.2, outperforming other models. For PM_{10}, the HR-PM-TS model achieves strong results, with an R^2 of 0.85, an RMSE of 3.73, an MAE of 1.70, and an M-Bias of -0.57. However, the M-Bias for PM_{10} is not the lowest among the models tested, and the difference in R^2 between HR-PM-TS and other models is less pronounced compared to $PM_{2.5}$. This discrepancy can be attributed to the primary sources of PM_{10}, which include local pollution sources such as road dust and construction sites [23-25]. These sources exhibit more complex and variable changes, making them harder to predict accurately. In contrast, the sources of $PM_{2.5}$, which include combustion processes, industrial emissions, etc. [26], tend to change more smoothly, allowing models to capture their patterns more effectively.

The stacking of base learners in the HR-PM-TS model enhances the network structure's complexity, leading to improved generalization for $PM_{2.5}$. According to Table 2, predicting $PM_{2.5}$ using HR-PM-TS takes only 18 minutes. In comparison, the computation time is significantly longer for other models: 223 minutes for RNN, 317 minutes for CNN, and 606 minutes for LSTM, making HR-PM-TS approximately 10-35 times faster. For PM_{10}, the computation times are 162 minutes for RNN, 300 minutes for CNN, and 122 minutes for LSTM, indicating that HR-PM-TS is 20-45 times faster in the prediction process. All experiments were conducted on a workstation equipped with an Intel(R) Xeon(R) Platinum 8383C CPU and 256GB of RAM, ensuring a robust and reliable evaluation of model performance.

Table 2. Comparison of Computation Time for $PM_{2.5}$ and PM_{10} Prediction Processes: HR-PM-TS vs. Deep Learning Models

	HR-PM-TS	RNN	CNN	LSTM
PM2.5	18min	223min	317min	606min
PM10	7min	162min	300min	122min

The HR-PM-TS demonstrates high predictive ability and strong generalization. For CAMS low-resolution grid data, linear interpolation is employed to obtain features at a resolution of 1 km × 1 km. The trained stacking model is then used to estimate high-resolution PM levels across these grids. This approach was applied to estimate the PM contributions for the year 2020 using the CAMS grid data. The average contributions of $PM_{2.5}$ and PM_{10} are illustrated in Figure 3, providing a detailed spatial distribution of PM levels at a high resolution.

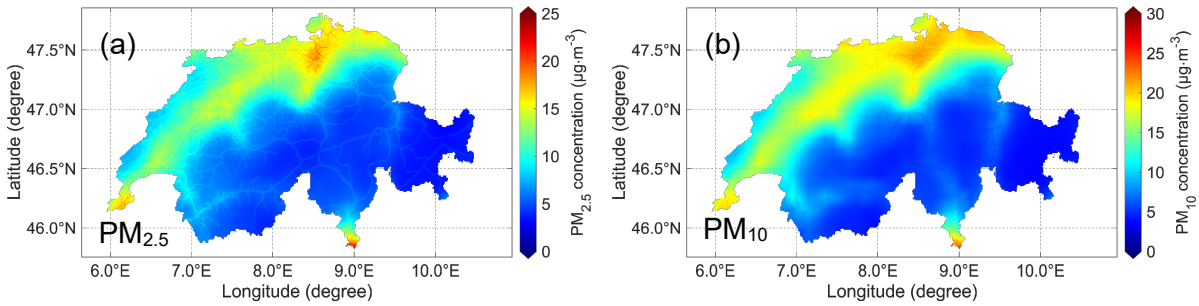

Figure 3. Average PM Contributions for the Year 2020: (a) $PM_{2.5}$ and (b) PM_{10}

3.2. Combine Estimated PM with Population

High-resolution PM data alone is not meaningful without considering the population distribution. According to the WHO Air Quality Guidelines 2021 [13], interim targets and Air Quality Guideline (AQG) levels for annual and 24-hour averages of $PM_{2.5}$ and PM_{10} are detailed in Table 3. Interim targets are defined as air pollutant levels that are higher than the AQG levels, serving as incremental steps towards achieving the ultimate AQG levels.

Table 3. The interim target and Air Quality Guideline (AQG) level

Pollutant	Averaging Time	Interim Target				Air Quality Guideline (AQG) Level
		1	2	3	4	
$PM_{2.5}$	Annual	35	25	15	10	5
	24-hour	75	50	37.5	25	15
PM_{10}	Annual	70	50	30	20	15
	24-hour	150	100	75	50	45

Referring to the four Interim target and AQG levels, PM concentrations are divided into five intervals. For each interval, the total population fraction and the population fractions of different age groups (Age 0-14, Age 15-64, Age 65+) are provided in Figure 4. As PM levels increase, the population fraction share increases to a maximum and then decreases.

For annual $PM_{2.5}$, the majority of the population fraction (Total: 0.49, Age 0-14: 0.50, Age 15-64: 0.49, Age 65+: 0.50) resides in interim target 3 (10-15 $\mu g/m^3$). In other interim targets and AQG levels, the population fractions across the three age groups are similar. The annual average $PM_{2.5}$ for each interval is also provided. For annual PM_{10}, the majority of the population fraction (Total: 0.52, Age 0-14: 0.52, Age 15-64: 0.52, Age 65+: 0.52) resides in interim target 4 (15-20 $\mu g/m^3$). The remaining population for PM_{10} is primarily within Interim Target 4, with a 0.89 total population fraction. This indicates that for $PM_{2.5}$, most of the population (0.73) exceeds the AQG level and interim target 4, whereas for PM_{10}, only 0.11 of the population exceeds the AQG level and interim target 4. The trends for the population fraction and PM concentrations differ between $PM_{2.5}$ and PM_{10}.

Age groups 0-14 and 65+ are considered more vulnerable to PM exposure. In the highest intervals for PM_{10} (Interim Target 3: 20-30 $\mu g/m^3$) and PM2.5 (Interim Target 2: 15-25 $\mu g/m^3$), the population fraction for Age 15-64 exceeds that of the more vulnerable age groups. This means that in the highest PM intervals, the exposure of vulnerable age groups is less than that of the Age 15-64 group. However, in Interim Targets 3 and 4 for $PM_{2.5}$, the population fractions of the vulnerable age groups (Interim Targets 3, Age 0-14: 0.50, Age 15-64: 0.49, Age 65+: 0.50) are equal to or greater than those of Age 15-64, indicating a greater exposure risk for the vulnerable age groups in these middle $PM_{2.5}$ intervals.

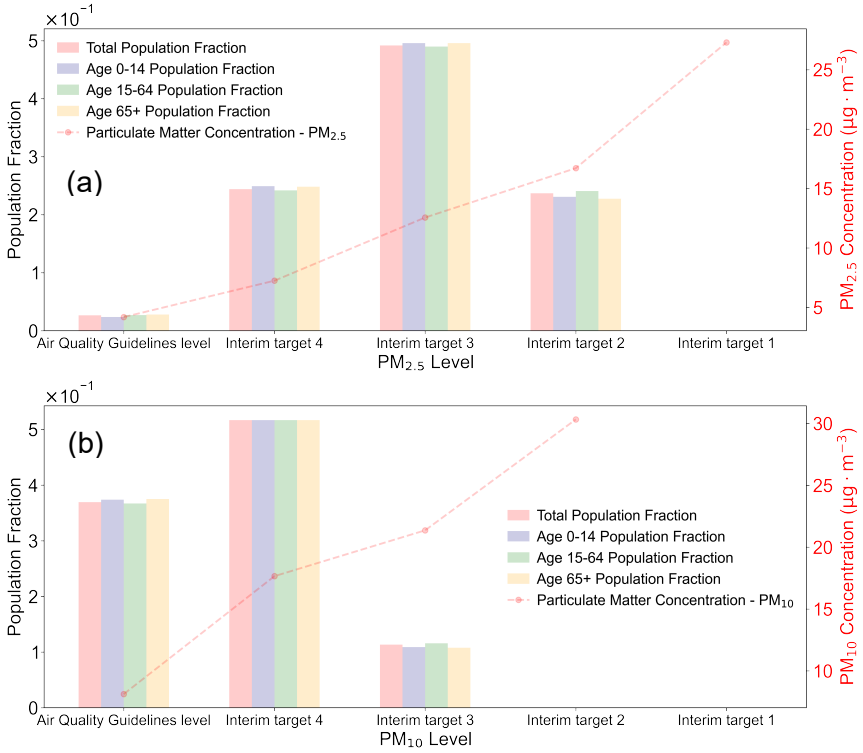

Figure 4. PM Level Intervals in Four Interim Targets and Air Quality Guideline (AQG) Levels by Age Groups (Age 0-14, Age 15-64, Age 65+): (a) $PM_{2.5}$ and (b) PM_{10} Annual Concentrations

To better integrate population data with PM levels, the 2020 annual weighted-population PM concentrations in 2686 administrative areas are presented in Figure 5: (a) $PM_{2.5}$ and (b) PM_{10}. For $PM_{2.5}$, when comparing weighted-population $PM_{2.5}$ to the unweighted $PM_{2.5}$: 66% of the administrative areas (1781 areas, with a maximum increase of 0.96 μg/m^3) show an increase. 26% of the areas (690 areas, with a maximum decrease of 1.13 μg/m^3) show a decrease. For PM_{10}, when comparing weighted-population PM_{10} to the unweighted PM_{10}: 56% of the administrative areas (1512 areas, with a maximum increase of 1.33 μg/m^3) show an increase. 33% of the areas (878 areas, with a maximum decrease of 1.34 μg/m^3) show a decrease. These results indicate that the majority of administrative areas experience an increase in PM levels when weighted by population, suggesting a higher exposure risk in more densely populated regions. This highlights the importance of considering population distribution in air quality assessments to better understand the actual exposure risk to the population.

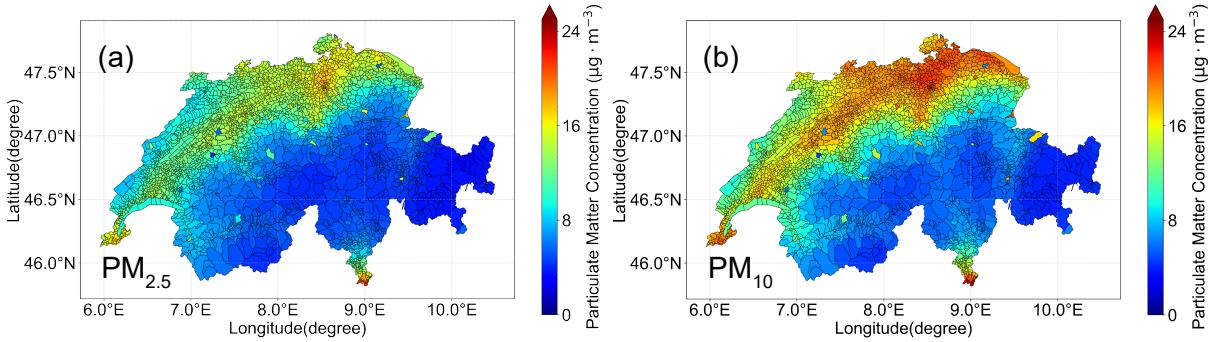

Figure 5. Annual Weighted Population PM Concentrations in Administration Areas: (a) $PM_{2.5}$ and (b) PM_{10}

3.3. Correlation Between Weighted-Population $PM_{2.5}$ and PM_{10} and Land Cover Types

To compare the weighted-population $PM_{2.5}$ and PM_{10} levels with various land cover types, correlation coefficients were analyzed and presented in Figure 6. The land cover types included Built-Up, Tree, Bare, Crops, Grass, Shrub, Moss/Lichen, Snow, Permanent Water, and Seasonal Water.

For $PM_{2.5}$, there was a significant positive correlation with areas categorized as Built-Up (correlation coefficient: 0.513, p-value < 0.001) and Crops (correlation coefficient: 0.512, p-value < 0.001). This indicates that regions with more Built-Up and Crops tend to have higher $PM_{2.5}$ concentrations, likely due to increased human activities such as transportation, industrial, and agricultural emissions [23, 27]. Conversely, significant negative correlations were found with Bare (correlation coefficient: -0.58, p-value < 0.001), Grass (correlation coefficient: -0.77, p-value: < 0.001), Shrub (correlation coefficient: -0.72, p-value: < 0.001), Moss/Lichen (correlation coefficient: -0.49, p-value < 0.001), and Snow (correlation coefficient: -0.25, p-value < 0.001). These negative correlations suggest that areas with more natural land cover types tend to have lower $PM_{2.5}$ concentrations, likely due to the natural filtration and particulate matter adsorption capabilities of these covers [28, 29]. For PM_{10}, the correlation patterns were similar to those observed for $PM_{2.5}$. Although the correlation with Tree cover was weak for both $PM_{2.5}$ (p-value > 0.05) and PM_{10}, it was statistically significant for PM_{10} (correlation coefficient: 0.042, p-value < 0.05), indicating a complex relationship that requires further study. The correlations with Permanent and Seasonal Water were weak but statistically significant for PM_{10} ($p < 0.01$; $p < 0.001$) and $PM_{2.5}$ ($p < 0.05$; $p < 0.01$).

In summary, areas with increased human activities (such as transportation, industrial, and agricultural activities) tend to have higher $PM_{2.5}$ and PM_{10} concentrations. Conversely, areas with more natural land cover types like grass, shrubs, and moss/lichen have lower concentrations of particulate matter due to their adsorption capacity and the settling effects of snow. Areas with higher levels of human activity and less natural cover are associated with increased concentrations of particulate matter, highlighting the impact of land use on air quality.

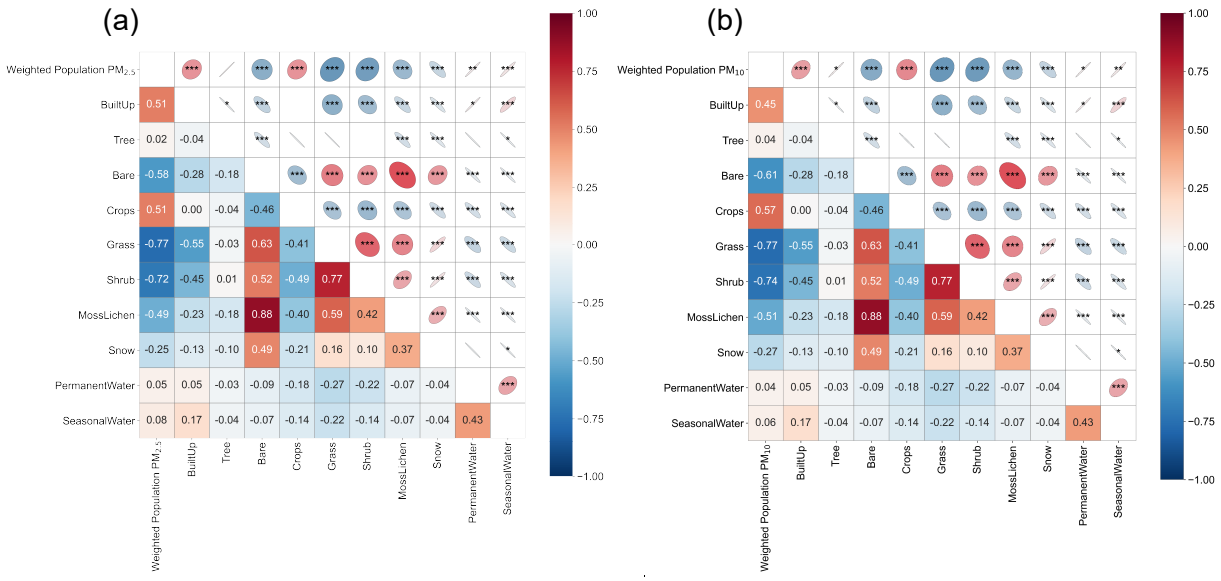

Figure 6. Correlation Heatmap of Annual Weighted Population PM Concentrations: (a) $PM_{2.5}$ and (b) PM_{10}

Table 4. Significance Levels (P-values) for 10 Land Cover Types for $PM_{2.5}$ and PM_{10}

Pollutant	**Land Cover Type**									
	Built-Up	Tree	Bare	Crops	Gras	Shrub	Moss/ Lichen	Snow	Permanent Water	Seasonal Water
$PM_{2.5}$	<0.001	0.22	<0.001	<0.001	<0.001	<0.001	<0.001	<0.001	<0.01	<0.001
PM_{10}	<0.001	<0.05	<0.001	<0.001	<0.001	<0.001	<0.001	<0.001	<0.05	<0.01

4. CONCLUSION

This study presents an innovative approach using the Stacking Method for enhanced data fusion in pollutant population risk evaluation, focusing on $PM_{2.5}$ and PM_{10}. And a high-resolution particulate matter estimation model (HR-PM-TS) is developed. The HR-PM-TS model demonstrated superior prediction accuracy and computational efficiency compared to traditional and deep learning models. Specifically, the model achieved an R^2 of 0.90, an RMSE of 2.14, and an MAE of 1.17 for $PM_{2.5}$, and an R^2 of 0.85, an RMSE of 3.73, and an MAE of 1.70 for PM_{10}. The model also reduced computation times significantly, with $PM_{2.5}$ predictions taking 18 minutes compared to 223 minutes for RNN, 317 minutes for CNN, and 606 minutes for LSTM, and PM_{10} predictions taking 7 minutes compared to 162 minutes for RNN, 300 minutes for CNN, and 122 minutes for LSTM. The model also significantly reduced computation times, with $PM_{2.5}$ predictions being approximately 20 times faster on average compared to other models (RNN, CNN, and LSTM). For PM_{10}, the predictions were roughly 30 times faster on average.

HR-PM-TS integrates population data with PM levels to better understand exposure risks across different regions and age groups. Our analysis, which references the four interim targets and AQG levels, revealed distinct trends for $PM_{2.5}$ and PM_{10} when considering population-weighted exposure. For $PM_{2.5}$, a significant portion of the population (0.73) resides in areas that exceed the AQG level and interim target 4, with 66% of administrative areas and a maximum increase of 0.96 μg/m^3, showing increased $PM_{2.5}$ levels after population weighting. This indicates a heightened exposure risk, especially in densely populated regions. In contrast, for PM_{10}, most of the population remains within the AQG levels and interim target 4, with only 11% of the population living in areas exceeding these levels. However, 56% of areas experienced increased PM_{10} levels when population-weighted with a maximum of 1.33 μg/m^3, although the trend differed from that of $PM_{2.5}$. These findings underscore the varying exposure risks posed by $PM_{2.5}$ and PM_{10}, highlighting the necessity of targeted air quality management strategies that consider both pollutant levels and population distribution. By examining the population fractions across different AQG intervals and age groups, the study emphasizes the increased exposure risk in densely populated regions, particularly for $PM_{2.5}$.

The correlation analysis between PM concentrations and land cover types indicated significant positive correlations for $PM_{2.5}$ with Built-Up (r = 0.51) and Crops (r = 0.51), suggesting higher $PM_{2.5}$ levels in areas with more human activities. Conversely, significant negative correlations were observed with Bare (r = -0.58), Grass (r = -0.77), Shrub (r = -0.72), Moss/Lichen (r = -0.49), and Snow (r = -0.25), indicating lower $PM_{2.5}$ levels in these areas due to their natural filtration capacities. Similar patterns were found for PM_{10}, with a notable weak but significant correlation for Permanent (r = 0.041) and Seasonal (r = 0.062) Water. The impact of land cover types on air quality, with urban and agricultural areas contributing to higher PM levels, while natural landscapes help reduce pollution. This underscores the importance of incorporating land cover considerations into air quality management strategies to effectively mitigate particulate matter pollution.

These findings are crucial for informing environmental and health policy development. The integration of high-resolution PM data with population distribution highlights the need for targeted air quality management strategies, particularly in densely populated and high-risk areas. By understanding the relationship between particulate matter, population distribution, and land cover, policymakers can devise more effective interventions to mitigate the impact of air pollution on public health.

Acknowledgements

This work is partially supported by the National Key Research and Development Program of China No.2023YFC3008803, and Independent Research Project Funding of China Institute for Radiation Protection ZFYHHJMN-2023001.

References

[1] Alexeeff SE, Liao NS, Liu X, Van Den Eeden SK, Sidney S. Long-Term PM(2.5) Exposure and Risks of Ischemic Heart Disease and Stroke Events: Review and Meta-Analysis. (2047-9980 (Electronic))

[2] Lelieveld J, Evans JS, Fnais M, Giannadaki D, Pozzer A. The contribution of outdoor air pollution sources to premature mortality on a global scale. (1476-4687 (Electronic))

[3] Vodonos A, Awad YA, Schwartz J. The concentration-response between long-term PM2.5 exposure and mortality; A meta-regression approach. Environmental Research 2018;166:677-89.http://doi.org/https://doi.org/10.1016/j.envres.2018.06.021

[4] Southerland VA, Brauer M, Mohegh A, Hammer MS, van Donkelaar A, Martin RV, et al. Global urban temporal trends in fine particulate matter (PM2.5) and attributable health burdens: estimates from global datasets. The Lancet Planetary Health 2022;6(2):e139-e46.http://doi.org/10.1016/S2542-5196(21)00350-8

[5] Lelieveld J, Evans JS, Fnais M, Giannadaki D, Pozzer A. The contribution of outdoor air pollution sources to premature mortality on a global scale. Nature 2015;525(7569):367-71.http://doi.org/10.1038/nature15371

[6] Shin M, Kang Y, Park S, Im J, Yoo C, Quackenbush LJ. Estimating ground-level particulate matter concentrations using satellite-based data: a review. GIScience & Remote Sensing 2020;57(2):174-89.http://doi.org/10.1080/15481603.2019.1703288

[7] Just AC, Arfer KB, Rush J, Dorman M, Shtein A, Lyapustin A, et al. Advancing methodologies for applying machine learning and evaluating spatiotemporal models of fine particulate matter (PM2.5) using satellite data over large regions. ATMOSPHERIC ENVIRONMENT 2020;239:117649.http://doi.org/https://doi.org/10.1016/j.atmosenv.2020.117649

[8] Ghahremanloo M, Choi Y, Sayeed A, Salman AK, Pan S, Amani M. Estimating daily high-resolution PM2.5 concentrations over Texas: Machine Learning approach. ATMOSPHERIC ENVIRONMENT 2021;247:118209.http://doi.org/https://doi.org/10.1016/j.atmosenv.2021.118209

[9] Chen W, Ran H, Cao X, Wang J, Teng D, Chen J, et al. Estimating PM2.5 with high-resolution 1-km AOD data and an improved machine learning model over Shenzhen, China. Science of The Total Environment 2020;746:141093.http://doi.org/https://doi.org/10.1016/j.scitotenv.2020.141093

[10] Zhang D, Du L, Wang W, Zhu Q, Bi J, Scovronick N, et al. A machine learning model to estimate ambient PM2.5 concentrations in industrialized highveld region of South Africa. Remote Sensing of Environment 2021;266:112713.http://doi.org/https://doi.org/10.1016/j.rse.2021.112713

[11] Danesh Yazdi M, Kuang Z, Dimakopoulou K, Barratt B, Suel E, Amini H, et al. Predicting Fine Particulate Matter (PM2.5) in the Greater London Area: An Ensemble Approach using Machine Learning Methods. *Remote Sensing.* 12. 2020.
[12] Yu W, Ye T, Zhang Y, Xu R, Lei Y, Chen Z, et al. Global estimates of daily ambient fine particulate matter concentrations and unequal spatiotemporal distribution of population exposure: a machine learning modelling study. The Lancet Planetary Health 2023;7(3):e209-e18.http://doi.org/10.1016/S2542-5196(23)00008-6
[13] Organization WH, others. WHO global air quality guidelines : particulate matter (PM2.5 and PM10), ozone, nitrogen dioxide, sulfur dioxide and carbon monoxide. World Health Organization; 2021.
[14] Meinshausen M, Jeffery L, Guetschow J, Robiou du Pont Y, Rogelj J, Schaeffer M, et al. National post-2020 greenhouse gas targets and diversity-aware leadership. Nature Climate Change 2015;5(12):1098-106.http://doi.org/10.1038/nclimate2826
[15] Huang X, Srikrishnan V, Lamontagne J, Keller K, Peng W. Effects of global climate mitigation on regional air quality and health. Nature Sustainability 2023;6(9):1054-66.http://doi.org/10.1038/s41893-023-01133-5
[16] Inness A, Ades M, Agustí-Panareda A, Barré J, Benedictow A, Blechschmidt AM, et al. The CAMS reanalysis of atmospheric composition. Atmos. Chem. Phys. 2019;19(6):3515-56.http://doi.org/10.5194/acp-19-3515-2019
[17] Muñoz-Sabater J. ERA5-Land hourly data from 1950 to present. In: (CDS) CCCSCSCDS, ed. Copernicus Climate Change Service (C3S) Climate Data Store (CDS); 2019.
[18] Center for International Earth Science Information Network CCU. Gridded Population of the World, Version 4 (GPWv4): Population Density Adjusted to Match 2015 Revision UN WPP Country Totals, Revision 11. Palisades, New York: NASA Socioeconomic Data and Applications Center (SEDAC); 2018.
[19] Buchhorn M, Smets B, Bertels L, Roo BD, Lesiv M, Tsendbazar N-E, et al. Copernicus Global Land Service: Land Cover 100m: collection 3: epoch 2 019: Globe. V3.0.1 ed.: Zenodo.
[20] Buchhorn M, Lesiv M, Tsendbazar N-E, Herold M, Bertels L, Smets B. Copernicus Global Land Cover Layers—Collection 2. *Remote Sensing.* 12. 2020.
[21] Pedregosa F, Varoquaux G, Gramfort A, Michel V, Thirion B, Grisel O, et al. Scikit-learn: Machine Learning in Python. Journal of Machine Learning Research 2011;12:2825-30
[22] Zhou Z-H. Machine Learning. Springer Singapore; 2021.
[23] Charron A, Harrison RM. Fine (PM2.5) and Coarse (PM2.5-10) Particulate Matter on A Heavily Trafficked London Highway: Sources and Processes. Environmental Science & Technology 2005;39(20):7768-76.http://doi.org/10.1021/es050462i
[24] Furusjö E, Sternbeck J, Cousins AP. PM10 source characterization at urban and highway roadside locations. Science of The Total Environment 2007;387(1):206-19.http://doi.org/https://doi.org/10.1016/j.scitotenv.2007.07.021
[25] Lin Z, Ji Y, Lin Y, Yang Y, Gao Y, Wang M, et al. PM10 and PM2.5 chemical source profiles of road dust over China: Composition, spatio-temporal distribution, and source apportionment. Urban Climate 2023;51:101672.http://doi.org/https://doi.org/10.1016/j.uclim.2023.101672
[26] McDuffie EE, Martin RV, Spadaro JV, Burnett R, Smith SJ, O'Rourke P, et al. Source sector and fuel contributions to ambient PM2.5 and attributable mortality across multiple spatial scales. Nature Communications 2021;12(1):3594.http://doi.org/10.1038/s41467-021-23853-y
[27] Fu Y, Tai APK, Liao H. Impacts of historical climate and land cover changes on fine particulate matter (PM2.5) air quality in East Asia between 1980 and 2010. Atmos. Chem. Phys. 2016;16(16):10369-83.http://doi.org/10.5194/acp-16-10369-2016
[28] Janhäll S. Review on urban vegetation and particle air pollution – Deposition and dispersion. ATMOSPHERIC ENVIRONMENT 2015;105:130-7.http://doi.org/https://doi.org/10.1016/j.atmosenv.2015.01.052
[29] Cai M, Xin Z, Yu X. Spatio-temporal variations in PM leaf deposition: A meta-analysis. Environmental Pollution 2017;231:207-18.http://doi.org/https://doi.org/10.1016/j.envpol.2017.07.105